LOW-SPEED LAYER IN WATER-COVERED AREAS*

FRANK PRESS† AND MAURICE EWING†

ABSTRACT

In many water-covered areas it has been reported that the speed of sound in the topmost layers of the bottom is less than that in water. Several methods of investigating such layers are discussed. The normal-mode theory offers the best method of detecting and investigating a low-speed layer covered by water.

INTRODUCTION

The surface layer on land, sometimes called the "weathered layer," always has a low sound velocity. Its depth is usually determined on land by a short refraction profile or by vertical shooting in a drill hole. Does this low velocity layer continue out to sea? If so, the short refraction profile is inadequate to determine it completely because of the higher sound velocity in water. The availability of boreholes for weathering determinations is likely to be much less than on land. The normal-mode theory of sound propagation, which was first introduced into the literature of seismology in a form appropriate for use in practical problems by Pekeris, probably offers the best method for detection and investigation of a low-velocity bottom. The studies of Ide, in which a constant-frequency sound source was used, have shown the sharp contrast between sound propagation over low-speed and over high-speed bottoms. Some evidence is given that soundings obtained from a conventional fathometer may often be a valuable adjunct.

OCCURRENCE OF LOW-SPEED BOTTOM

Osterhoudt's paper[1] brought to the attention of the authors the importance of the question of whether the "weathered" layer extends out under the ocean, a question which was probably clearly in the minds of people in seismic work who were approcahing the beach from the landward side. He reported depths up to 1,000 feet with velocity 3,800 ft/sec in South Timbalier Bay and adjacent waters of the Gulf of Mexico.

Ewing and Worzel[2] found that the dispersion in the water wave at two stations just off the delta of the Orinoco River was radically different from that found off the east coast of the United States and off several Caribbean islands. It will be shown later that this can be explained by the presence of low-velocity bottom.

* This work represents results of research carried out for the Bureau of Ships of the Navy Department under contract with Columbia University. Manuscript received by the Editor March 15, 1948.

† Department of Geology, Columbia University, New York.

[1] Walter J. Osterhoudt, "The Seismograph Discovery of an Ancient Mississippi River Channel," *Geophysics*, XI (1946), 417.

[2] Maurice Ewing and J. L. Worzel, *Memoir 27, Geological Society of America* (in press).

The refraction travel-time curves in this offshore work seldom have observations at less than about one-half mile, but even these curves showed the probability of low-velocity bottom at the Orinoco Stations.

Ide, Post and Fry[3] working in the mouth of the Potomac River, have found abundant evidence that the sound velocity in the bottom is lower than that in water in the summer time.

Several investigators,[4,5,6] making fathometer surveys, have found a reflecting surface beneath the bottom giving an echo so strong, relative to the echo from the bottom, that it is almost certain that the intervening layer has low sound velocity.

These occurrences support the plausible hypothesis that the low-velocity bottom is most likely to be found in areas of rapid deposition.

METHODS OF INVESTIGATION

Shooting in bore holes.—Any of the conventional methods of "weathering" determination based on bore holes would probably work as well at sea as on land, but one reason for preparing the present paper is that there probably will never be many bore holes available at sea.

Refraction time-distance curve.—Typical records from short refraction shots at sea in a region of high-velocity bottom are shown in Figure 1*A* and *B*. The time-distance curve derived from these and related records is shown in Figure 2. The seismograms show the first arrivals to be low-frequency waves which have come through the ground. They are followed by an abrupt arrival of high-frequency sound, which marks the beginning of the water wave. At practically every station investigated, the high-frequency sound in the water wave arrives superposed on ground waves, and because of dispersion, shows a gradual decrease in frequency.

In all of our work the water-wave travel time has been used to give the distance to the shotpoint, assuming the speed of sound in water derived from the temperature and salinity of the water. The water wave has always been readily distinguished by its high-frequency character and, at short or moderate distances by its high amplitude. In the time-distance curves the unit of distance is usually taken, for the sake of convenience, as the distance sound travels through water in one second, so that all water-wave arrivals would plot on a line whose slope is unity.

In Figure 2 the ground waves arrive ahead of the water waves and plot on a line through the origin whose slope indicates a sound velocity 5,900/4,925 times

[3] J. M. Ide, R. F. Post, and W. S. Fry, "The Propagation of Underwater Sound at Low Frequencies as a Function of the Acoustic Properties of the Bottom," Naval Research Laboratory Report S-2113(August, 1943).

[4] K. T. Adams, *Hydrographic Manual*, Special Publication No. 143, U. S. Coast and Geodetic Survey (1946), p. 571.

[5] F. L. Peacock, Season's Report, U. S. Coast and Geodetic Survey Archives, Project No. 248, Gulf of Maine (1940), 15 pages.

[6] H. W. Murray, "Topography of the Gulf of Maine—Field Season 1940," *Bulletin Geological Society of America, 58* (1947), 153–196.

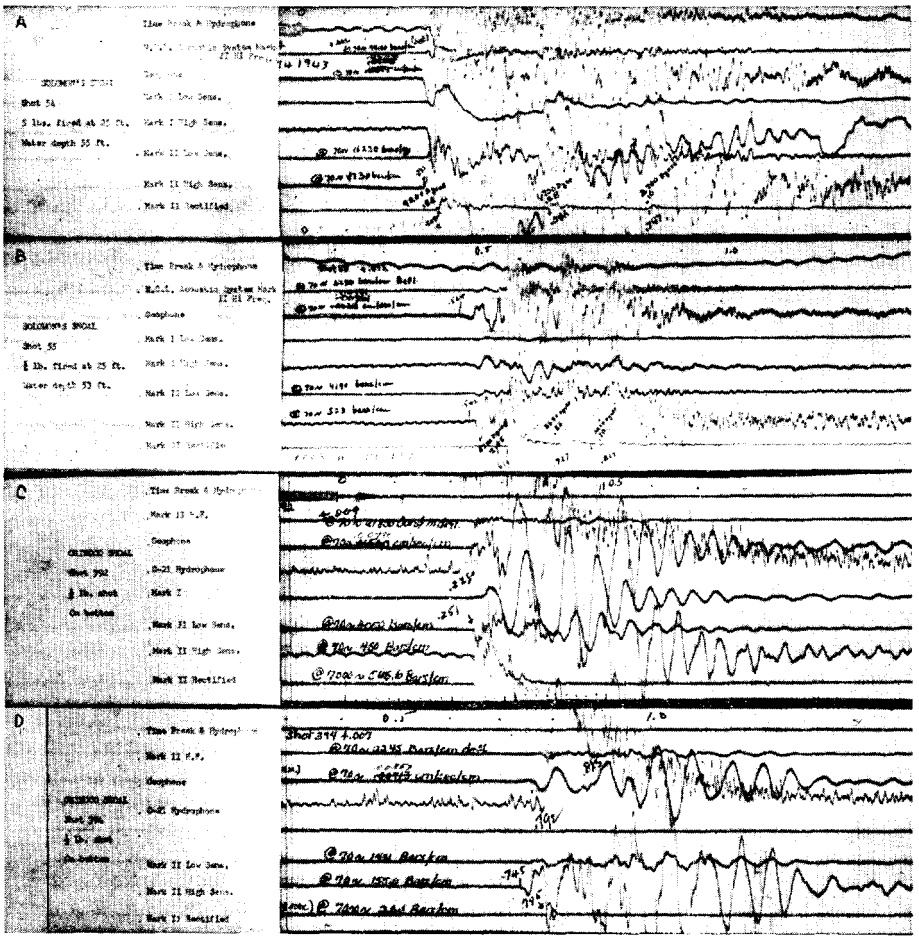

FIG. 1. Typical records from short refraction shots at sea in a region of high-velocity bottom (*A* and *B*) and in a region of low-velocity bottom (*C* and *D*).

greater than that in water. Such data are conclusive evidence that the velocity of sound in the bottom is greater than that in the water by the amount indicated. In all cases where this type of time-distance curve has been found, the dispersion in the water wave gives concordant information about the bottom.

In Figure 1, *C* and *D* are typical records from short-refraction shots at sea in a region of low-velocity bottom. The time-distance curve for these and the related shots is shown in Figure 3. The seismograms show the first arrival to be high-frequency sound for record *C*, which is at the shortest distance. For longer shots, as typified by record *D*, the low-frequency ground waves arrive first, but they plot on a line which passes well above the origin, with an intercept of 0.09 sec.

On the basis of the standard theory[7] for interpretation of refraction profiles, the presence of the intercept and the absence of a ground-wave arrival on record *C* indicate that the first layer of the ocean bed has a sound velocity less than that of water. Study of the relative amplitudes in the four records of Figure 1 leaves little hope that the arrival of a ground wave, similar to the first arrival of *A* and *B*, could be identified if it arrived shortly after the water wave. On the basis of the

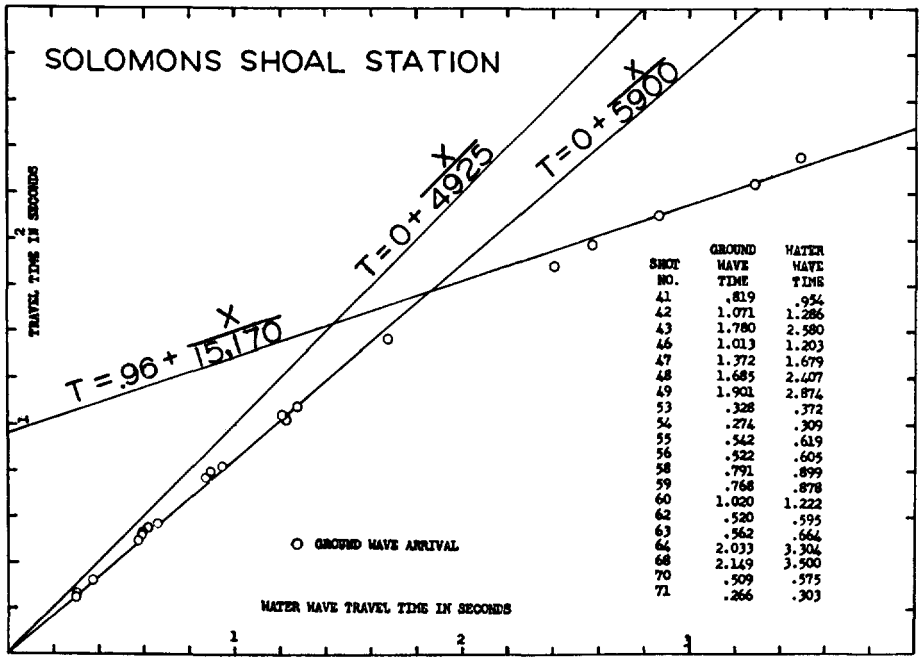

FIG. 2. Typical time-distance curve in a region of high-velocity bottom.

standard theory, if the ground waves in Figure 3 corresponding to the low-velocity layers could be identified, the thickness H of this layer would be given by

$$H = V_2 T_3 / 2 \cos \alpha \qquad (1)$$

where V_2 is the velocity of sound in the second layer (first layer of the bottom), $\alpha = \sin^{-1} V_2/V_3$ with V_3 the velocity of the third layer (second layer of the bottom), and T_3 the intercept of the V_3-branch of the travel-time curve. Thus the depth can be computed only if the velocity V_2 is known from some independent measurement.

[7] See for instance: Maurice Ewing, G. P. Woollard, and A. C. Vine, "Geophysical Investigations in the Emerged and Submerged Atlantic Coastal Plain, Part III: Barnegat Bay, New Jersey, Section," *Bull. Geol. Soc. of Amer.*, *50* (1939), 257–296.

The standard interpretation has been that the water waves are of high frequency because the water is a superior elastic medium which passes all frequencies well. The low frequency of the ground waves has been explained on the basis of imperfections in the elasticity of the earth, which discriminated strongly against the high frequencies through absorption. The contrast between this view and that based on the normal-mode theory will be pointed out in a later section.

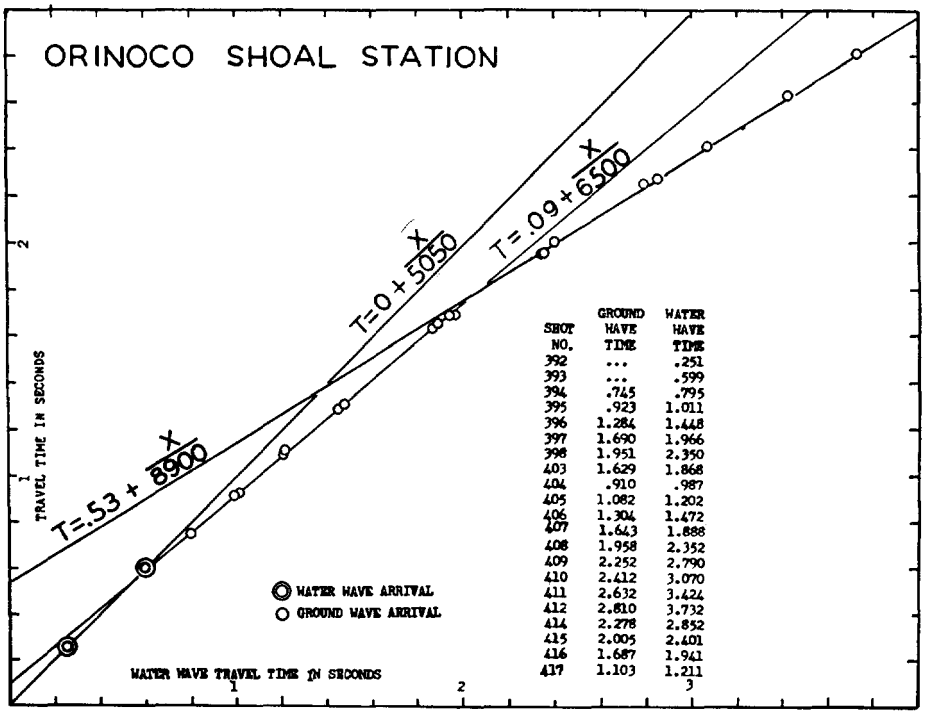

FIG. 3. Typical time-distance curve in a region of low-velocity bottom.

Soundings.—Examples of localities in which a fathometer receives an echo from some surface beneath the bottom have been reported by several investigators, for example, Adams[8] (1946). Murray[9] (1947) gives many beautiful examples in the Gulf of Maine of the dual bottom feature, mainly in depressions (Fig. 4). He attributes this to sedimentation on an older surface, and states that in many cases the reflection from the first bottom was much weaker than that from the second. He states further that the sedimentation areas are generally found in basins at depths greater than about 80 fathoms and that the sediment ranges in thickness

[8] *Op. cit.*, p. 571.
[9] *Loc. cit.*

from a thin film up to about 90 feet. There is no evidence in the fathometer readings alone whether the velocity in the sediment is greater or less than that in water, only that the reflection coefficient at the water-sediment interface is small compared to that between the sediment and the older surface which is presumably the crystalline basement.

A. P. Crary, in a personal communication, has reported that in 1942, using a

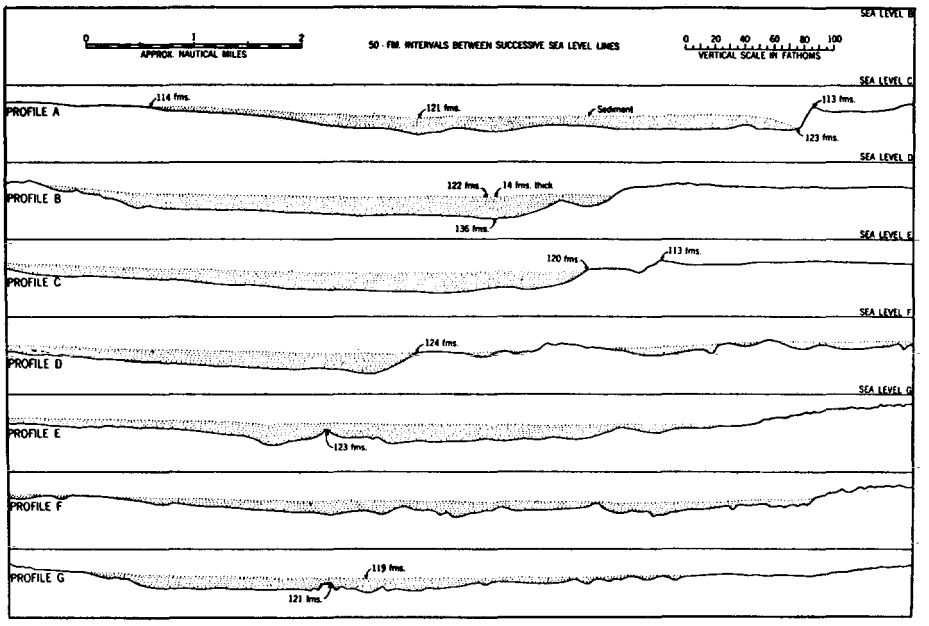

FIG. 4. Composite tracings of Hughes Veselekari fathograms crossing Rodger Basin, Gulf of Maine. (U. S. Coast & Geodetic Survey.)

fathometer in the mouths of the Mississippi River, he noted a second bottom at a depth of some 70 fathoms.

It is of some interest to note that if s_2 is the travel time indicated by the fathometer or other method for vertical travel from the ocean bottom to the reflecting lower surface, then we may put $2H = V_2 s_2$ into (1), obtaining the values V_2 and H from

$$\begin{aligned} s_2 &= T_3/\cos\alpha, \\ H &= V_2 s_2/2. \end{aligned} \tag{2}$$

Thus if s_2 is measured with a fathometer or by vertical seismic reflections, and V_3 and T_3 are measured from a refraction profile, H and V_2 may be calculated. The precision of this measurement of V_2 would be low because it involves the difference $(s_2^2 - T_3^2)$, a small quantity.

Calculation of the relative intensities of sounds reflected at normal incidence from the dual bottoms yields results which may provide geological conclusions of some interest.

From Rayleigh[10] the ratio R of reflected to incident amplitude for normal incidence at the interface between two liquids of densities ρ_1 and ρ_2 and sound velocities V_1 and V_2 is

$$R = (\rho_2/\rho_1 - V_1/V_2)(\rho_2/\rho_1 + V_1/V_2)^{-1}. \tag{3}$$

It may be noted that the absolute value of the reflection coefficient at a given interface for normal incidence is unchanged when the direction of approach is reversed.

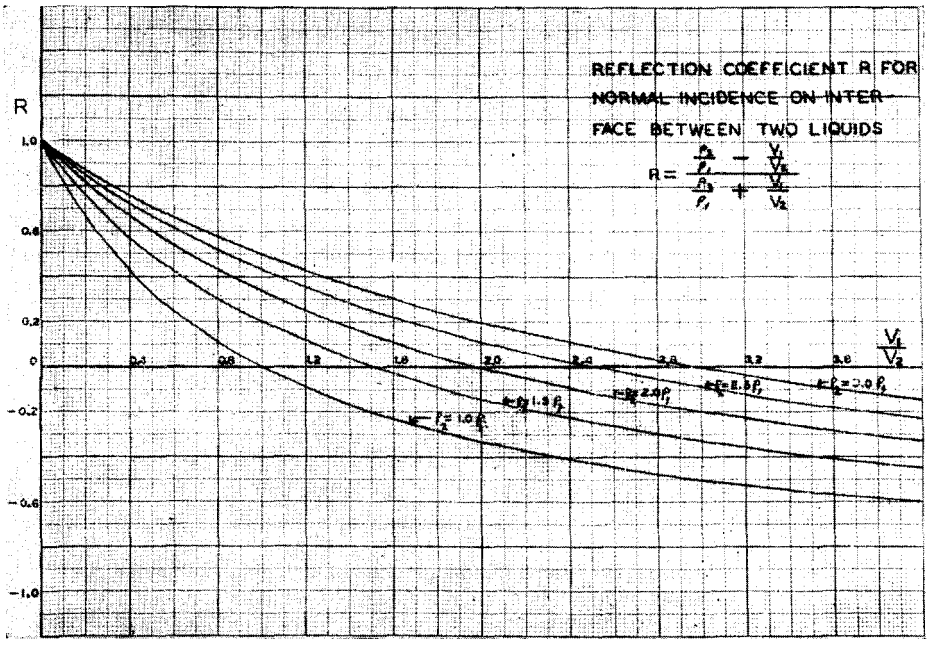

FIG. 5. Reflection coefficient R for normal incidence on interface between two liquids plotted as a function of velocity contrast for various density ratios.

Figure 5 is a plot of reflection coefficient as a function of velocity contrast for various densities. On the supposition that ρ_2/ρ_1, is between 1.0 and 3.0 at the bottom, it is seen from the graph that R can be small only when V_1/V_2 is of the same order of magnitude, which indicates a low velocity bottom ($V_1 > V_2$). The large reflections from the lower interface observed by Murray therefore point strongly to a layer of mud, whose velocity is less than that of water, underlain by crystal-

[10] Lord Rayleigh, *Theory of Sound*, II, Macmillan, 1926, 82.

line rock whose velocity is several times greater. This discussion is valid only for wave lengths small compared with the thickness of the layer.

Dispersion in water waves from explosions—High-velocity bottom.—Pekeris[11] has given the theory of normal-mode propagation for two and three liquid layers of

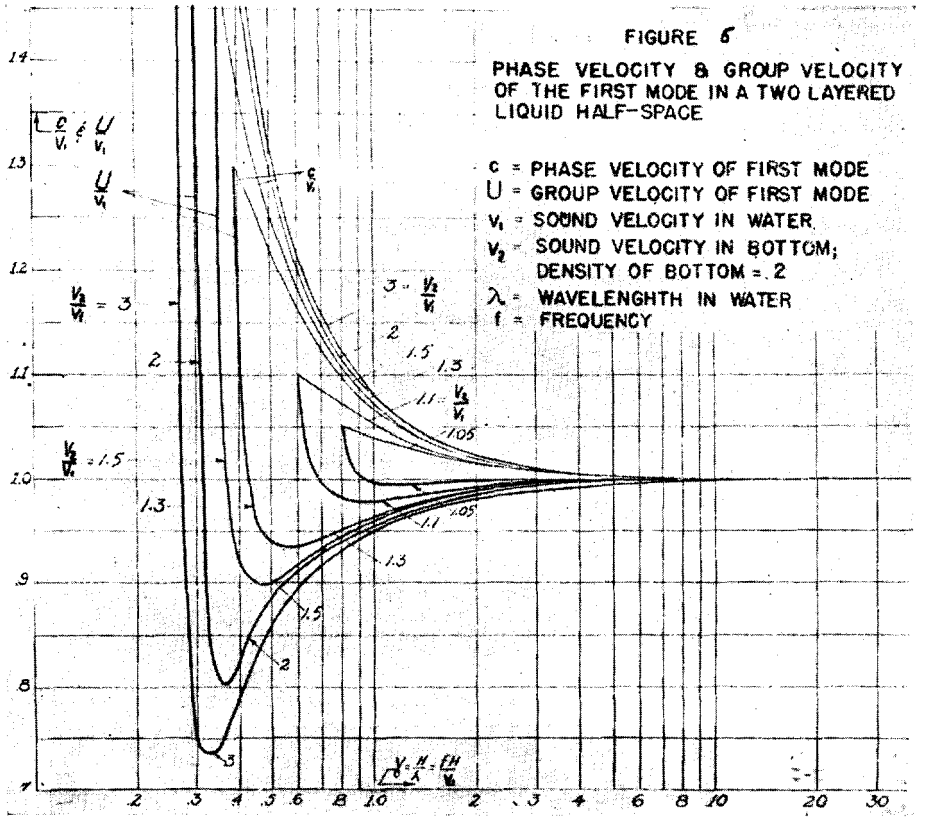

FIG. 6. Phase and group-velocity curves for normal-mode sound propagation in two liquid layers. (After Pekeris.)

successfully higher velocity. For the two layer case his results may be summarized by the family of phase-velocity and group-velocity curves plotted in Figure 6, with the acoustic properties of the layers as parameters.

A typical sequence of signals received from a distant explosion in shallow water is shown in Figure 7. This may be explained by referring to any one of the group-velocity curves of Figure 6. The first arrivals, corresponding to the extreme left end of the group-velocity curve, are low-frequency waves which have

[11] C. L. Pekeris, *Memoir 27, Geological Society of America* (in press).

travelled through the ground with velocity V_2. These are followed by waves with slowly increasing frequency which are abruptly interrupted by high-frequency waves, which arrive at the time corresponding to a velocity V_1. These high frequencies correspond to the extreme right-hand end of the group-velocity curve. Their frequency rapidly decreases until the time corresponding to the group-velocity minimum, at which time the frequency is the same as that approached by

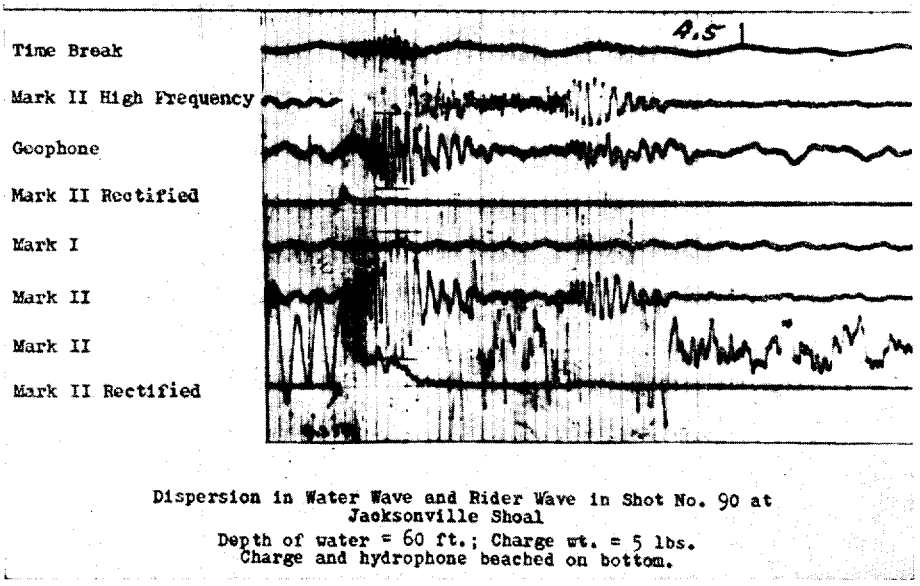

FIG. 7. Water-wave and portion of ground-wave arrival from a distant explosion in shallow water.

the earlier low-frequency waves. Waves corresponding to the part of the group-velocity curve to the right of the minimum will be called water waves, those corresponding to the left part of the curve will be called ground waves. These distinctions strictly apply only to the two ends of the group-velocity curve, and ground transmission gradually changes into water transmission at the minimum. Pekeris has named the frequency corresponding to the minimum of group velocity the Airy frequency and this part of the seismogram the Airy phase.

The Airy phase is characterized by large amplitudes which become the most prominent features of the seismograms at greater distances. The earlier part of the seismogram is usually affected by arrivals which have travelled through deeper, higher-speed layers. Thus the simple two-layer theory given above usually applies only to that part of the seismogram fairly near the water-wave arrivals, but the theory will account for that part of the seismogram in great detail.

In Pekeris' three-layer theory, the water waves behave much as they do for

the two-layer case, provided the second layer is several times thicker than the first.

Dispersion in water waves from explosions—Low-velocity bottom.—Calculations have been made for the phase and group velocity in case the bottom is composed of a low-velocity layer, $V_2 < V_1$ underlain by a high-velocity layer, $V_3 > V_1$. These curves are shown in Figure 8 to consist of two branches. The first is much like

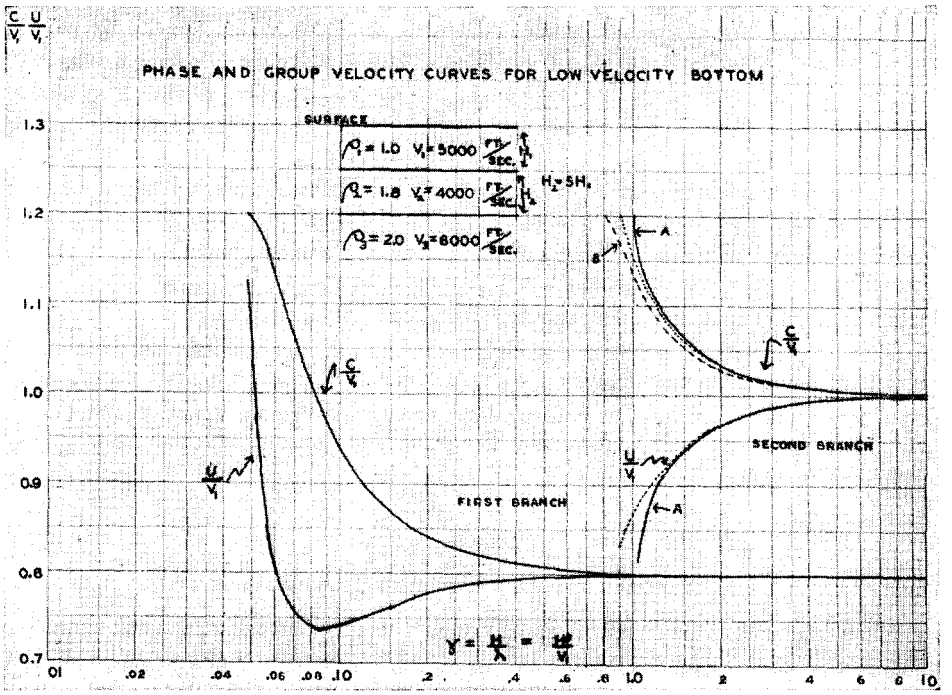

FIG. 8. Phase and group-velocity curves for normal-mode sound propagation in three liquid layers. The intermediate layer represents the low-velocity bottom.

those of Figure 6 and can be discussed in a similar manner. The high frequencies should now arrive with a velocity V_2 appropriate to the low-speed layer instead of travelling with the speed of sound in water. At the time corresponding to the group velocity $U = V_3$, the waves arrive with the cutoff frequency. At the time corresponding to the minimum-group velocity, the Airy phase should arrive, and it should be the most prominent phase on the record. However, only that part of the group-velocity curve to the left of the minimum has as yet been observed. The failure to find the high-frequency part of the signal, and the Airy phase, travelling with velocities in the neighborhood of that for mud, is attributed to absorption phenomena in the mud, and possibly to stratification in the mud.

The second branch, in Figure 8, consists of two parts, A and B, and is dis-

tinguished by the absence of a minimum-group velocity. High-frequency waves will arrive with the velocity of sound in water. The lower frequencies will be highly attenuated because of loss of energy into the bottom. Branch II represents a type of propagation which is essentially characterized by multiple reflections in the water layer. The reflection coefficient for a ray incident on a low-velocity bottom increases with the angle of incidence. It approaches total reflection for grazing incidence, hence only those rays having grazing incidence will be propagated without severe loss of energy. It will be shown in the appendix that these rays contain only the very high frequencies. The occurrence of water waves consisting only of a brief burst of high-frequency sound is typical of the stations discussed in this paper, and is considered the best evidence for the existence of low-velocity bottom.

Ide's method of constant frequency.—Ide[12] used a continuous-sound source of constant frequency mounted on a ship. The sound receiver was in the water, or on the bottom, or in the mud beneath the bottom. He measured the vertical and horizontal variation in intensity at various frequencies, in the range of frequency where the wave length is comparable to the depth of the water.

He established the existence of normal-mode propagation for both hard and soft bottoms, by means of several types of measurement. Since he was dealing with a continuous sound, he had no need to consider group velocity. Details of this work are given in reports of the Naval Research Laboratory, and Ide is now preparing them for publication.

APPENDIX

DERIVATION AND DISCUSSION OF THE PERIOD EQUATIONS

The complete theory of sound propagation in three liquid layers was given by Pekeris,[13] who solved the problem for spherical waves originating at an impulsive point source. Pekeris did not examine the case for which the intermediate layer has a lower sound velocity than the first layer. The complete solution for the case of a low-velocity bottom can be obtained from the Pekeris theory, but it is sufficient for our purposes to discuss the solution for plane waves. The plane-wave solution results in the identical period equation given by Pekeris, and has the added advantage of giving an elementary picture of normal-mode propagation. For a rigorous derivation of the amplitudes and periods of sound waves originating in shallow-water explosions, one must use the methods of Pekeris.

Let us consider the propagation of plane sound waves in three liquid layers having densities ρ_1, ρ_2, ρ_3, sound velocities V_1, V_2, V_3, and thicknesses h_1, h_2, and ∞, respectively. The cartesian coordinate system is chosen so that the xy-plane lies in the free surface, with x oriented in the direction of propagation, and the z-axis vertically downward. We introduce the sound potential $\phi(x, z, t)$ related to

[12] *Loc. cit.*

[13] *Loc. cit.*

the pressure p and the horizontal and vertical particle velocities u and w by the equations:

$$p = \rho\partial\phi/\partial t, \qquad u = \partial\phi/\phi x, \qquad w = \partial\phi/\phi z. \tag{1}$$

It is required to find functions ϕ_j which satisfy the wave equations

$$\partial^2/\phi_j/\partial t^2 = V_j{}^2\nabla^2\phi_j; \qquad j = 1, 2, 3. \tag{2}$$

It can readily be verified that solutions are of the form:

$$\left.\begin{aligned}
&(a)\quad \phi_1 = A \exp\left[\eta_1 z\right] \exp\left[i(kx - \omega t)\right] \\
&\qquad\quad + B \exp\left[-\eta_1 z\right] \exp\left[i(kx - \omega t)\right], \\
&(b)\quad \phi_2 = C \exp\left[\eta_2 z\right] \exp\left[i(kx - \omega t)\right] \\
&\qquad\quad + D \exp\left[-\eta_2 z\right] \exp\left[i(kx - \omega t)\right], \\
&(c)\quad \phi_3 = E \exp\left[-\eta_3 z\right] \exp\left[i(kx - \omega t)\right],
\end{aligned}\right\} \tag{3}$$

where η_3 is real and positive.

The function ϕ_3 is taken to decrease exponentially with depth since we are interested in the case where no energy is lost by refraction into the lowest layer. This is equivalent to postulating that only sound waves which are totally reflected at the lowest interface are considered in the solution. Substituting equations (3) in (2) gives the following relations:

$$\left.\begin{aligned}
\eta_1 &= k(1 - C^2/V_1{}^2)^{1/2}, \\
\eta_2 &= k(1 - C^2/V_2{}^2)^{1/2}, \\
\eta_3 &= k(1 - C^2/V_3{}^2)^{1/2}.
\end{aligned}\right\} \tag{4}$$

In these equations the phase velocity C is related to the wave number k and the angular frequency ω by the equation $C = \omega/k$.

Equations (3) must satisfy boundary conditions which require the continuity of pressure and vertical particle velocity at the liquid interface, and zero pressure at the free surface. Thus we have

$$\left.\begin{aligned}
&\text{at } z = 0, && \rho_1\partial\phi_1/\partial t = 0; \\
&\text{at } z = h_1, && \rho_1\partial\phi_1/\partial t = \rho_2\partial\phi_2/\partial t; \\
& && \partial\phi_1/\partial z = \partial\phi_2/\partial z \\
&\text{at } z = h_1 + h_2, && \rho_2\partial\phi_2/\partial t = \rho_3\partial\phi_3/\partial t, \\
& && \partial\phi_2/\partial z = \partial\phi_3/\partial z.
\end{aligned}\right\} \tag{5}$$

Substituting equations (3) in (5) and eliminating the constants A, B, C, D, E between the resultant expressions yields the period equation:

$$\left.\begin{aligned}&(\rho_1/\rho_2)(1-C^2/V_2^2)^{1/2}(1-C^2/V_1^2)^{-1/2}\tanh\left[kh_1(1-C^2/V_1^2)^{1/2}\right]\\&\quad+\left\{(\rho_2/\rho_3)(1-C^2/V_3^2)^{1/2}(1-C^2/V_2^2)^{-1/2}\right.\\&\qquad\qquad\left.\cdot\tanh\left[kh_2(1-C^2/V_2^2)^{1/2}\right]+1\right\}\\&\times\left\{(\rho_2/\rho_3)(1-C^2/V_3^2)^{1/2}(1-C^2/V_2^2)^{-1/2}\right.\\&\qquad\qquad\left.+\tanh\left[kh_2(1-C^2/V_2^2)^{1/2}\right]\right\}^{-1}=0.\end{aligned}\right\}\qquad(6)$$

For the low-speed bottom $V_2<V_1<V_3$. It is also required that $C<V_3$ in order for η_3 to be real, and we have therefore the two cases:

$$\text{I:}\quad V_2<C<V_1<V_3,$$

$$\text{II:}\quad V_2<V_1<C<V_3,$$

for which (6) reduces to:

Case I.

$$\left.\begin{aligned}&(\rho_1/\rho_2)(C^2/V_2^2-1)^{1/2}(1-C^2/V_1^2)^{-1/2}\tanh\left[kh_1(1-C^2/V_1^2)^{1/2}\right]\\&\quad+\left\{(\rho_2/\rho_3)(1-C^2/V_3^2)^{1/2}(C^2/V_2^2-1)^{-1/2}\right.\\&\qquad\qquad\left.\cdot\tan\left[kh_2(C^2/V_2^2-1)^{1/2}\right]+1\right\}\\&\times\left\{(\rho_2/\rho_3)(1-C^2/V_3^2)^{1/2}(C^2/V_2^2-1)^{-1/2}\right.\\&\qquad\qquad\left.-\tan\left[kh_2(C^2/V_2^2-1)^{1/2}\right]\right\}^{-1}=0.\end{aligned}\right\}\qquad(7)$$

Case II.

$$\left.\begin{aligned}&(\rho_1/\rho_2)(C^2/V_2^2-1)^{1/2}(C^2/V_1^2-1)^{-1/2}\tan\left[kh_1(C^2/V_1^2-1)^{1/2}\right]\\&\quad+\left\{(\rho_2/\rho_3)(1-C^2/V_3^2)^{1/2}(C^2/V_2^2-1)^{-1/2}\right.\\&\qquad\qquad\left.\cdot\tan\left[kh_2(C^2/V_2^2-1)^{1/2}\right]+1\right\}\\&\times\left\{(\rho_2/\rho_3)(1-C^2/V_3^2)^{1/2}(C^2/V_2^2-1)^{-1/2}\right.\\&\qquad\qquad\left.-\tan\left[kh_2(C^2/V_2^2-1)^{1/2}\right]\right\}^{-1}=0.\end{aligned}\right\}\qquad(8)$$

In Figure 9, *ADFGHI* represents the ray path of a plane wave which is reflected at the free surface, refracted into the second layer, and reflected at the interface of the second and third layer. As the wave front (shown by the dashed line) moves a distance $BC=V_1$ in unit time, a point on the wave front moves a distance JK in the horizontal direction, where $JK=C=V_1/\sin\theta_1=V_2/\sin\theta_2$ and C is the phase velocity. In this representation the wave number k is given by $k=(2\pi/\lambda_1)\sin\theta_1=(2\pi/\lambda_2)\sin\theta_2$, where λ_1 and λ_2 are the wave lengths measured along the ray paths in layers 1 and 2 respectively.

In general a fraction of the wave will be reflected each time the ray crosses the intermediate interface. If we denote the reflection coefficients for waves incident upon the interface from above and below by R_{12} and R_{21} respectively, we have from Rayleigh[14]

[14] *Op. cit.*, p. 81.

$$\left.\begin{aligned} R_{12} &= (\rho_2/\rho_1 - \cot\theta_2/\cot\theta_1)(\rho_2/\rho_1 + \cot\theta_2/\cot\theta_1)^{-1}; \\ R_{21} &= (\rho_1/\rho_2 - \cot\theta_1/\cot\theta_2)(\rho_1/\rho_2 + \cot\theta_1/\cot\theta_2)^{-1} = -R_{12}. \end{aligned}\right\} \quad (9)$$

Using the relationships $k(C^2/V_1^2-1)^{1/2}=(2\pi/\lambda_1)\cos\theta_1$, and $k(C_2^2/V_2^2-1)^{1/2}=(2\pi/\lambda_2)\cos\theta_2$ the previous equations become

$$\begin{aligned} R_{12} &= [\rho_2/\rho_1 - (C^2/V_2^2 - 1)^{1/2}(C^2/V_1^2 - 1)^{-1/2}] \\ &\quad \cdot [\rho_2/\rho_1 + (C^2/V_2^2 - 1)^{1/2}(C^2/V_1^2 - 1)^{-1/2}]^{-1} \\ &= -R_{21}. \end{aligned} \quad (10)$$

For Case I where $V_2<C<V_1<V_3$, R_{21} becomes complex and reduces to $R_{21}=\exp.\ [-i\psi_{21}]$, where $\tan(\psi_{21}/2)=(\rho_2/\rho_1)\ (1-C^2/V_1^2)^{1/2}\ (C^2/V_2^2-1)^{-1/2}$. The complex reflection coefficient indicates that total reflection with a phase change of $-\psi_{21}$ occurs for a ray incident on the first layer from below. Case I therefore represents a type of propagation in which the rays are confined to the low-velocity layer because of total reflection at the boundaries of this layer.

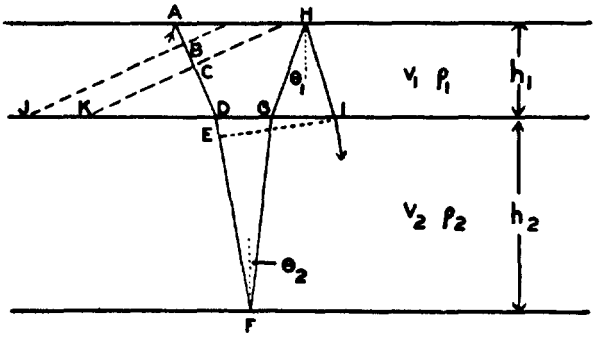

FIG. 9. Ray diagram of normal-mode sound propagation for the case of a low-velocity bottom.

In Case II the rays are confined to the first two layers due to total reflection at the free surface with a phase change of $-\pi$, and total reflection at the lowest interface with a phase change of $-\psi_{23}$ where $\tan(\psi_{23}/2)=(\rho_2/\rho_3)\ (1-C^2/V_3^2)^{1/2}\cdot(C^2/V_2^2-1)^{-1/2}$.

The period equation for sound propagation in two or three liquid layers is simply the condition for constructive interference between the rays which are multiply reflected at the various boundaries. This can be readily shown when $R_{12}=0$ or $(\rho_2/\rho_1)\ (C^2/V_1^2-1)^{1/2}\ (C^2/V_2^2-1)^{-1/2}=1$, that is, for the case when no partial reflection occurs at the interface between the first and second layers (Fig. 9).

If the wave front EI is to interfere constructively with the coincident wave front which has traversed the additional path $EFGHI$, it is required that:

$$(2\pi/\lambda_2)EFG - \psi_{23} + (2\pi/\lambda_1)GHI - \pi = 2(n-1)\pi \quad n = 1, 2, 3, \cdots \quad (11)$$

where $-\psi_{23}$ and $-\pi$ are the phase changes that occur at the lowest interface and free surface respectively. From the geometry of Figure 9 we note that:

$$GHI = 2h_1/\cos\theta_1;$$

$$EFG = 2h_2/\cos\theta_2 - (2h_2\tan\theta_2 + 2h_1\tan\theta_1)\sin\theta_2.$$

Substituting for GHI and EFG and using $\lambda_2/\lambda_1 = \sin\theta_1/\sin\theta_2$, equation (11) becomes:

$$(2\pi/\lambda_1)h_1\cos\theta_1 = -(2\pi/\lambda_2)h_2\cos\theta_2 + \psi_{23}/2 + (2n-1)\pi/2. \qquad (12)$$

Now

$$(2\pi/\lambda_1)\cos\theta_1 = k(C^2/V_1^2 - 1)^{1/2}, \qquad (2\pi/\lambda_2)\cos\theta_2 = k(C^2/V_2^2 - 1)^{1/2},$$

$$\tan(\psi_{23}/2) = (\rho_2/\rho_3)(1 - C^2/V_3^2)^{1/2}(C^2/V_2^2 - 1)^{-1/2}.$$

If we take the tangent of both sides of (12) and make these substitutions, the following equation is obtained:

$$\begin{aligned}&\tan\left[kh_1(C^2/V_1^2-1)^{1/2}\right]\\ &= -\left\{(\rho_2/\rho_3)(1-C^2/V_3^2)^{1/2}(C^2/V_2^2-1)^{-1/2}\tan\left[kh_2(C^2/V_2^2-1)^{1/2}\right]+1\right\}, \qquad (13)\\ &\times\left\{(\rho_2/\rho_3)(1-C^2/V_3^2)^{1/2}(C^2/V_2^2-1)^{-1/2}-\tan\left[kh_2(C^2/V_2^2-1)^{1/2}\right]\right\}^{-1}.\end{aligned}$$

This is the same as the period equation for Case II except for the amplitude factor $(\rho_1/\rho_2)(C^2/V_2^2-1)^{1/2}(C^2/V_1^2-1)^{-1/2}$, which is equal to unity for $R_{12}=0$. In general when $R_{12}\neq 0$, the amplitude factor enters into the period equation which represents the condition for constructive interference between three or more rays having different amplitudes depending upon the reflection coefficient at the intermediate interface.

The period equations (7) and (8) give the frequency $f=\omega/2\pi=Ck/2\pi$ as a function of the phase velocity with the dimensions and acoustic properties of the system as parameters. The equations cannot be solved explicitly for the frequency which must be determined by numerical calculations. It is found that the frequency is a multiple-valued function of the phase velocity, each value belonging to the various modes of two distinct branches. Each branch of the period equation corresponds to a different type of wave propagation.

The numerical calculations of the branches are simplified by making several changes in variables. We let $h_2=5h_1$ and

$$e = (\rho_2/\rho_3)(1 - C^2/V_3^2)^{1/2}(C^2/V_2^2 - 1)^{-1/2},$$

$$b = 5(C^2/V_2^2 - 1)^{1/2},$$

$$\Phi = kh_1a,$$

$$a = (1 - C^2/V_1^2)^{1/2} \text{ for Case I},$$

$$a = (C^2/V_1^2 - 1)^{1/2} \text{ for Case II},$$

$$f = (\rho_1/a\rho_2)(C^2/V_2^2 - 1)^{1/2}.$$

With these substitutions, equations (7) and (8) become:

Case I.

$$\tanh\Phi = \left\{e\tan\left[(b/a)\Phi\right] + 1\right\}\left\{f\left[\tan\left[(b/a)\Phi\right] - e\right]\right\}^{-1}. \qquad (14)$$

Case II.

$$\tan \Phi = \{e \tan [(b/a)\Phi] + 1\}\{f[\tan [(b/a)\Phi] - e]\}^{-1}. \qquad (15)$$

The numerical procedure is to choose a value of C/V_1, thus determining a, b, e, and f. Approximate values of Φ which satisfy (14) or (15) are obtained by successive trials. The correct value of Φ is obtained from the intersection of the graphs of the right and left sides of the period equation plotted as functions of Φ. Using the relationship $kh_1 = \Phi/a$, kh_1 and $\gamma = h_1/\lambda_1 = (kh_1C)/(2\pi V_1)$ are readily obtained. The group velocity $U = C + (kh_1)dC/d(kh_1)$ is determined by numerical differentiation.

The phase and group velocities of the first and second branches have been plotted as functions of γ in Figure 8. Branch I is obtained by calculating the smallest values of Φ which satisfy equations (14) and (15) for a chosen sequence of values of C/V_1. Higher modes of Branch I, representing transmission at higher frequencies, can be obtained by taking successively larger roots for the given sequence of (C/V_1) values. For all modes of Branch I, however, $\Phi \to 0$ as $C \to V_1$, in such a manner that $\Phi/a = kh_1$ remains finite. It can be seen from equations (7) and (8) that for the first branch, Case I grades continuously into Case II as C goes through V_1 (the first term in both equations approaches the same limit as $C \to V_1$).

The type of propagation represented by the first branch is now apparent. As C goes from V_3 to V_1 (Case II), the energy is distributed in the first two layers as multiply reflected rays which interfere constructively with each other. As $C \to V_1$, or as the frequency increases, the energy is drawn into the low-speed layer. For $C < V_1$ (Case I) the propagation consists of multiply reflected rays confined to the low-speed layer. The energy for this case is concentrated in the low-speed layer and falls off exponentially with distance from the boundaries of this layer. If equation (3a) is substituted in the first boundary condition, it is found that $A = -B$, and $\phi_1 = 2a \sinh(\eta_1 z) \exp[i(kx - \omega t)]$. From equation (4) it is seen that the rates, η_1 and η_3, at which the velocity potentials ϕ_1 and ϕ_3 decrease with distance from the boundaries of the low-speed layer, increase as C approaches V_2 or as the frequency increases.

Branch II consists of two parts, A and B, both of which are obtained from equation (15) (Case II) by determining the values of Φ corresponding to a given sequence of values C/V_1, such that $\Phi \to \pi$ as $C \to V_1$. In Branch IIA $\Phi \geqq \pi$ whereas $\Phi \leqq \pi$ for Branch IIB. Branch II represents a type of propagation for which the rays are confined to the first two layers. However, the functional dependence of phase and group velocity on frequency is essentially determined by propagation in the first layer. This can be seen by writing down the condition for constructive interference of rays confined to the first layer because of total reflection with a phase change of $-\pi$ at the free surface and partial reflection at the intermediate interface.

$$(2\pi/\lambda_1)h_1 \cos \theta_1 - \pi = 2(n-1)\pi \quad n = 1, 2, 3, \cdots. \qquad (16)$$

We also have $C = V_1/\sin\theta_1$ and from (16)

$$U = C - \lambda dc/d\lambda = V_1 \sin\theta_1. \tag{17}$$

A plot of C/V_1 and U/V_1 as functions of γ based on the previous equations is shown by the dotted curve of Figure 8. The close fit with Branch II, especially for higher frequencies, is apparent.

The rays confined to the first layer will in general have small amplitudes because of partial refraction into the second layer at each reflection from the intermediate interface. With increasing angles of incidence corresponding to decreasing C or increasing f, the reflection coefficient R_{12} increases in absolute value and approaches unity for grazing incidence. The energy of the waves represented by the second branch is therefore drawn into the first layer with increasing frequency. It is to be expected, therefore, that a signal propagated according to the second branch would appear as a high frequency burst arriving with a velocity $U = V_1$. The lower-frequency arrivals would not be observed because of their small amplitudes. This characteristic arrival pattern has been observed and is described in an earlier section.